Anal. Chem. **2001,** *73,* 2261−2267

Scanning Electrochemical Microscopy. 41. Theory and Characterization of Ring Electrodes

Youngmi Lee, Shigeru Amemiya, and Allen J. Bard*

Department of Chemistry and Biochemistry, University of Texas at Austin, Austin, Texas, 78712

Ring ultramicroelectrodes, which are of particular interest as probes for scanning electrochemical microscopy (SECM), combined with near-field scanning optical microscopy, were investigated. Theoretical SECM tip current−distance (approach) curves for a ring electrode were calculated by numerical (finite element) analysis. The SECM curves obtained were a function of the geometry of the tips including the thickness of the ring and the insulating sheath. Theoretical approach curves over conductive substrates showed a strong dependence on the ratio of inner to outer radii of ring microelectrodes (a/b) and were relatively insensitive to the thickness of the insulating sheath (r_g). For insulating substrates, however, the approach curves varied significantly with r_g, but much less with the a/b ratio. Comparison of experimental and theoretical SECM curves provided a good method of evaluating the size and shape of ring electrodes. Good agreement of the experimental and theoretical curves was found with a ring microelectrode with a nominal 200-nm ring thickness, yielding values of 1.7, 1.9, and 5.7 μm for the inner (a) and outer (b) radii of a ring and the outermost radius of insulating sheath (r_g), respectively.

Although planar disk-shaped microelectrodes have been used most frequently as tips in scanning electrochemical microscopy (SECM),[1,2] the use of microelectrodes possessing other geometries, for example, shaped as cones,[3,4] hemispheres,[3−6] or spheres,[5,7] and the corresponding theoretical expressions for the SECM tip current, i_T, as a function of tip−substrate distance, d, have been reported. These investigations for nonplanar microelectrodes are important since the construction of spherical or conical-shaped microelectrodes is often easier than disk-shaped microelectrodes, especially for very small tips.[3,8−15]

The first theoretical study of the SECM feedback response was accomplished only for disk-shaped tips using a finite element method (FEM).[16] Analytical approximations were obtained later for $i_T - d$ curves in SECM with nonplanar tips, such as hemispherical or conical.[3] More accurate studies of SECM responses with tip geometry have been performed using numerical simulations based on the boundary element method (BEM)[4,5] and the alternating direction implicit finite difference method (ADIFDM).[6]

Ring-shaped electrodes are of special interest in connection with optical fiber probes, since the electrode can be fashioned by depositing metal on the shaft of the fiber, insulating the layer, and polishing the end. Such ring-shaped microelectrodes have been used as an SECM probe in optical microscopy experiments, although no approach curves were shown.[17−19] Similar ring microelectrodes were previously used for photoelectrochemical microscopy (PEM)[17−19] and photoelectrochemical experiments.[20,21] We have been especially interested in combining SECM with near-field scanning optical microscopy (NSOM). In this technique, the probe is usually constructed by pulling an optical fiber to a sharp (∼100-nm-diameter) tip and coating the outside wall of the fiber with aluminum. To produce a useful electrode, one must replace the Al with a noble metal, such as gold, and insulate the shaft by coating it with an appropriate material and polishing the tip end. This results in a tip with a ring-shaped gold electrode that has the optical fiber core in its center. We have obtained experimental SECM approach curves for both conductive and insulating substrates with such a ring electrode for the first time. Details about the preparation of such ring microelectrodes and their application in optical microscopy experiments will be reported elsewhere.[22]

Despite several reports of SECM with ring electrodes, there have been no descriptions of the theory of SECM response with a ring-shaped tip. We report here the first study of the steady-state SECM tip current as a function of tip−substrate distance at a ring microelectrode and compare the results to the theoretical

(1) Bard, A. J.; Fan, F.-R.; Mirkin, M. V. In *Electroanalytical Chemistry: A Series of Advances*; Bard, A. J., Ed.; Marcel Dekker: New York, 1994; Vol. 18, p 243.
(2) *Scanning Electrochemical Microscopy*; Bard, A. J., Mirkin, M. V., Eds.; Marcel Dekker: New York, 2001.
(3) Mirkin, M. V.; Fan, F.-R. F.; Bard, A. J. *J. Electroanal. Chem.* **1992**, *328*, 47.
(4) Fulian, Q.; Fisher, A. C.; Denuault, G. *J. Phys. Chem. B* **1999**, *103*, 4387.
(5) Fulian, Q.; Fisher, A. C.; Denuault, G. *J. Phys. Chem. B* **1999**, *103*, 4393.
(6) Selzer, Y.; Mandler, D. *Anal. Chem.* **2000**, *72*, 2383.
(7) Demaille, C.; Brust, M.; Tsionsky, M.; Bard, A. J. *Anal. Chem.* **1997**, *69*, 2323.
(8) Lee, C.; Miller, C. J.; Bard, A. J. *Anal. Chem.* **1991**, *63*, 78.
(9) Fan, F.-R. F.; Bard, A. J. *Science* **1995**, *267*, 871.
(10) Fan, F.-R. F.; Bard, A. J. *Science* **1995**, *270*, 1849.
(11) Fan, F.-R. F.; Kwak, J.; Bard, A. J. *J. Am. Chem. Soc.* **1996**, *118*, 9669.
(12) Forouzan, F.; Bard, A. J. *J. Phys. Chem. B* **1997**, *101*, 10876.
(13) Fan, F.-R. F.; Bard, A. J. *Proc. Natl. Acad. Sci. U.S.A.* **1999**, *96*, 14222.
(14) Slevin, C. J.; Gray, N. J.; Macpherson, J. V.; Webb, M. A.; Unwin, P. R. *Electrochem. Commun.* **1999**, *1*, 282.
(15) Gray, N. J.; Unwin, P. R. *Analyst* **2000**, *125*, 889.
(16) Kwak, J.; Bard, A. J. *Anal. Chem.* **1989**, *61*, 1221.
(17) Casillas, N.; James, P.; Smyrl, W. H. *J. Electrochem. Soc.* **1995**, *142*, L16.
(18) James, P.; Casillas, N.; Smyrl, W. H. *J. Electrochem. Soc.* **1996**, *143*, 3853.
(19) Shi, G.; Garfias-Mesias, L. F.; Smyrl, W. H. *J. Electrochem. Soc.* **1998**, *145*, 2011.
(20) Kuhn, L. S.; Weber, A.; Weber, S. G. *Anal. Chem.* **1990**, *62*, 1631.
(21) Pennarun, G. I.; Boxall, C.; O'Hare, D. *Analyst* **1996**, *121*, 1779.
(22) Lee, Y.; Bard, A. J., in preparation.

10.1021/ac0014764 CCC: $20.00
Published on Web 04/10/2001

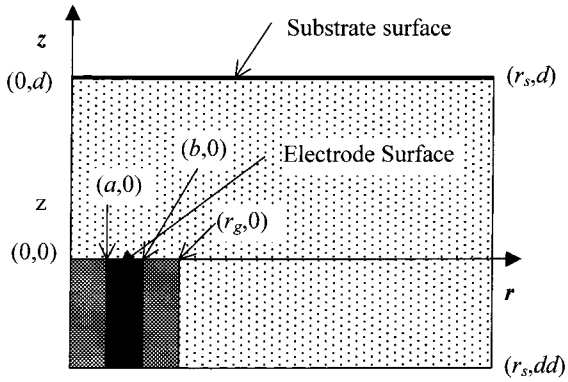

Figure 1. Diagram of a ring electrode in cylindrical coordinates.

response. The numerical solution of the partial differential equations was carried out with PDEase2D, a commercial program employing finite element analysis.[23] The comparison of theoretical SECM approach curves with experimental ones provided information about tip geometry including the ratio of inner and outer ring radii (a/b) and the thickness of the insulating sheath (r_g) (see Figure 1).

EXPERIMENTAL SECTION

Materials. $Ru(NH_3)_6Cl_3 \cdot 10H_2O$ was obtained from Strem Chemicals. KCl (EM Industries, Inc.) was used as a supporting electrolyte. All solutions were prepared with 18 MΩ cm^{-1} deionized water with reagent grade compound without further purification.

Electrochemical and SECM Experiments. For electrochemical experiments, a three-electrode system was used. The working electrode was the ring electrode, the counter electrode was a Pt wire, and the reference electrode was Ag/AgCl. The ring electrode was a pulled optical fiber surrounded with a deposited gold layer, with electrophoretic paint as the external insulator. The construction procedure for such ring electrodes is described elsewhere.[22] A CH Instruments (Austin, TX) model 900 SECM and a home-built SECM were used to perform all cyclic voltammetry and SECM measurements. Instrumentation and techniques for SECM experiments were similar to those described in previous publications.[16,24,25] Flat glass and platinum sheets were used as substrates for the SECM approach experiments. The surface of the platinum substrate was polished successively with 0.3-, 0.1-, and 0.05-μm alumina using polishing cloth before each experiment. For SECM approach curves, the movement of the electrode toward the substrate was stopped before the electrode contacted the substrate surface (glass or platinum) to avoid damage to the tip. Thus, the end points of data in all experimental SECM curves shown are not the contact point but the point at which tip approach was stopped.

THEORY OF RING ELECTRODES IN SECM

When the ring electrode is far from the substrate, the diffusion to the small electrode rapidly achieves hemispherical diffusion at steady state (but hemitoroidal at short times). However, when it is positioned in close proximity (i.e., within a few radii) to a flat substrate, the diffusion is affected by the substrate and shows different responses depending on the geometry of the tip.[3] Since the first theoretical treatment of the SECM response at disk electrode,[16] there have been several contributions on the SECM response with different kinds of tip geometries, such as hemispheres and cones.[6,23] No previous treatment of ring-shape ultramicroelectrodes has been reported.

Here we describe the steady-state tip current as a function of distance between a tip and a substrate at a ring microelectrode studied using a numerical solution of relevant equations. A diagram for a thin-ring electrode is shown in Figure 1.

First, we considered a following simple electron-transfer reaction at the ring electrode surface.

$$\mathrm{O} + n\mathrm{e}^- \underset{k_b}{\overset{k_f}{\rightleftharpoons}} \mathrm{R} \tag{1}$$

where k_f and k_b are heterogeneous electron-transfer rate constants. The concentration of species O is denoted as $c(r,z,t)$ and the diffusion equation in cylindrical coordinates is described as

$$\frac{\partial c}{\partial t} = D\left(\frac{\partial^2 c}{\partial r^2} + \frac{1}{r}\frac{\partial c}{\partial r} + \frac{\partial^2 c}{\partial z^2}\right) \tag{2}$$

where r and z are the coordinates in directions parallel and normal to the electrode surface, respectively. D is the diffusion coefficient, and c is the concentration of O. For convenience, normalized dimensionless variables are introduced as follows.

$$R = r/b \tag{3a}$$

$$Z = z/b \tag{3b}$$

$$C = c(r,z,t)/c_0 \tag{3c}$$

$$L = d/b \tag{3d}$$

$$\mathrm{LL} = dd/b \tag{3e}$$

$$\mathrm{RI} = a/b \tag{3f}$$

$$\mathrm{RG} = r_g/b \tag{3g}$$

$$\mathrm{RS} = r_s/b \tag{3h}$$

where a and b are, respectively, the inner and outer radii of the ring, c_0 is the bulk concentration of O, d is the tip−substrate separation, dd is the distance to the simulation limit behind the tip surface, r_g is the outermost electrode radius, and r_s is the space limit.

Since we are only interested in the steady-state system, the following diffusion equation was used for the calculations.

$$\frac{\partial C}{\partial t} = \frac{\partial^2 C}{\partial R^2} + \frac{1}{R}\frac{\partial C}{\partial R} + \frac{\partial^2 C}{\partial Z^2} = 0 \quad \text{at steady state} \tag{4}$$

The digital simulation for a ring SECM probe was performed by calculating the diffusion-controlled steady-state current i_T at different tip−substrate distances, d (over substrates).

(23) Mirkin, M. V. In *Scanning Electrochemical Microscopy*; Bard, A. J., Mirkin, M. V., Eds.; Marcel Dekker: New York, 2001; Chapter 4.
(24) Bard, A. J.; Fan, F.-R. F.; Kwak, J.; Lev, O. *Anal. Chem.* **1989**, *61*, 132.
(25) Kwak, J.; Bard, A. J. *Anal. Chem.* **1989**, *61*, 1794.

The mixed boundary conditions are given by the following at steady state: For a conductive substrate,

$$\partial C(0,Z)/\partial R = 0 \quad \text{for} \quad 0 \le Z < L \tag{5}$$

$$\partial C(RG,Z)/\partial R = 0 \quad \text{for} \quad \mathrm{LL} \le Z < 0 \tag{6}$$

$$\partial C(R,0)/\partial Z = 0 \quad \text{for} \quad 0 \le R < RI \quad \text{or for} \quad 1 \le R < \mathrm{RG} \tag{7}$$

$$C(\mathrm{RS},Z) = 1 \quad \text{for} \quad \mathrm{LL} \le Z < L \tag{8}$$

$$C(R,\mathrm{LL}) = 1 \quad \text{for} \quad \mathrm{RG} \le R < \mathrm{RS} \tag{9}$$

$$C(R,0) = 0 \quad \text{for} \quad \mathrm{RI} \le R < 1 \tag{10}$$

$$C(R,L) = 1 \quad \text{for} \quad 0 \le R < \mathrm{RS} \tag{11a}$$

and for an insulating substrate,

$$\partial C(R,L)/\partial Z = 0 \quad \text{for} \quad 0 \le R < \mathrm{RS} \tag{11b}$$

The tip current for a whole surface of a ring electrode can be obtained as a function of tip−substrate distance.

$$i_T(L) = nFDc_0 b \int_{\mathrm{RI}}^{1} 2\pi R(\partial C/\partial Z)_{Z=0}\,\mathrm{d}R \tag{12}$$

Finally, the tip current was normalized to give, $I_T = i_T(L)/i_{T,\infty}$ where $i_{T,\infty}$ is the tip current when the electrode is located far from the substrate. The numerical solution of the diffusion equation was carried out with the program PDEase2D (Macsyma Inc., Arlington, MA).[23]

RESULTS AND DISCUSSION

Steady-State Diffusion-Limited Current. To characterize the SECM response, the limiting currents of ring ultramicroelectrodes in bulk solution are needed, because tip currents are usually normalized by the $d \rightarrow \infty$ limiting currents. Many contributions have been devoted to the theory of the diffusion-controlled steady-state current at a ring microelectrode ($i_{T,\infty}$). Szabo[26] and Fleischmann et al.[27−29] calculated $i_{T,\infty}$ with the assumption of uniform accessibility to the surface of the ring microelectrode of an arbitrary thickness, although exact numerical analysis of the surface current density distribution shows that this assumption is not true. Phillips and Stone[30] extended this study of $i_{T,\infty}$ to the region where the electrode reaction rate is not diffusion controlled with no assumptions other than that the thickness of the ring is much thinner than the overall ring radius. Smythe[31] calculated the theoretical $i_{T,\infty}$ considering nonuniform accessibility for a thin ring and this result, in eq 13, has been regarded as the most accurate.

Table 1. Normalized Steady-State Current[a] at Ring Microelectrodes

b/a	Smythe[b]	Cooke[c]	Szabo[c]	our results[d]
∞		4	4	4.007
2		3.924	3.917	3.914
1.5		3.798	3.801	3.789
1.25	3.575	3.590	3.596	3.579
1.20	3.500	3.510	3.516	3.511
1.125	3.326	3.330	3.335	3.333
1.0909	3.202	3.204	3.208	3.194
1.0213	2.667	2.667	2.668	2.642

[a] $l_0/b = i_{T,\infty}/nFDcb$. [b] Calculated using eq 14. [c] From ref 26. [d] Calculated for RG = 100.

$$i_{T,\infty} = nFDcl_0 \tag{13}$$

$$l_0 = [\pi^2(a+b)]/\ln[16(a+b)/(b-a)] \quad \text{when} \quad b/a < 1.25 \tag{14}$$

where n is the number of electrons, F is the Faraday constant, D is the diffusion coefficient, c is the concentration of electroactive species, a is the inner ring radius, and b is the outer ring radius.

All above treatments assume that the insulating sheath is infinitely thick. As reported for disk microelectrodes,[32−35] a thinner insulating sheath produces an enhanced $i_{T,\infty}$ because of additional diffusion of the electroactive species from behind the electrodes.[36,37] First, we simulated $i_{T,\infty}$ with infinite RG and compared the results obtained at a given l_0/b, with those of previous reports to confirm the accuracy of our simulation method. Table 1 shows that our results agree well (within 0.06−0.98%) with previous results. The RG effect on $i_{T,\infty}$ for ring microelectrodes was also studied. As reported for disk microelectrodes,[32−35] $i_{T,\infty}$ of ring microelectrodes is enhanced as the thickness of the insulating sheath decreases. For example, when $a/b = 0.95$, the values of l_0/b obtained were 3.341, 3.086, 3.005, and 2.944 for RG = 1.5, 3, 5, and 10, respectively.

SECM Approach Curves for Ring Microelectrodes. At various normalized distances between an electrode and a substrate (L), the normalized tip current was calculated to obtain SECM approach curves for ring electrodes. The geometry of the ring electrodes is described by three parameters: inner radius (a), outer radius (b), and thickness of insulating sheath (r_g). To characterize the SECM response of ring electrodes depending on inner and outer radii, simulated SECM curves were obtained with a varying a/b ratio while keeping RG fixed. Figure 2 shows theoretical SECM feedback responses of ring electrodes when RG = 5. Compared to disk electrodes ($a/b = 0$), ring electrodes must approach closer to the substrate to reach a similar value of

(26) Szabo, A. *J. Phys. Chem.* **1987**, *91*, 3108.
(27) Fleischmann, M.; Bandyopadhyay, S.; Pons, S. *J. Phys. Chem.* **1985**, *89*, 5537.
(28) Pons, S.; Fleischmann, M. *Anal. Chem.* **1987**, *59*, 1391A.
(29) Fleischmann, M.; Pons, S. *J. Electroanal. Chem.* **1987**, *222*, 107.
(30) Phillips, C. G.; Stone, H. A. *J. Electroanal. Chem.* **1995**, *396*, 277.
(31) Smythe, W. R. *J. Appl. Phys.* **1951**, *22*, 1499.
(32) Shao, Y.; Mirkin, M. V. *J. Phys. Chem. B* **1998**, *102*, 9915.
(33) Dayton, M. A.; Brown, J. C.; Stutts, K. J.; Wightman, R. M. *Anal. Chem.* **1980**, *52*, 946.
(34) Shoup, D.; Szabo, A. *J. Electroanal. Chem.* **1984**, *160*, 27.
(35) Fang, Y.; Leddy, J. *Anal. Chem.* **1995**, *67*, 1259.
(36) Saraceno, R. A.; Ewing, A. G. *J. Electroanal. Chem.* **1988**, *257*, 83.
(37) Cope, D. K.; Tallman, D. E. *J. Electroanal. Chem.* **1995**, *396*, 265.

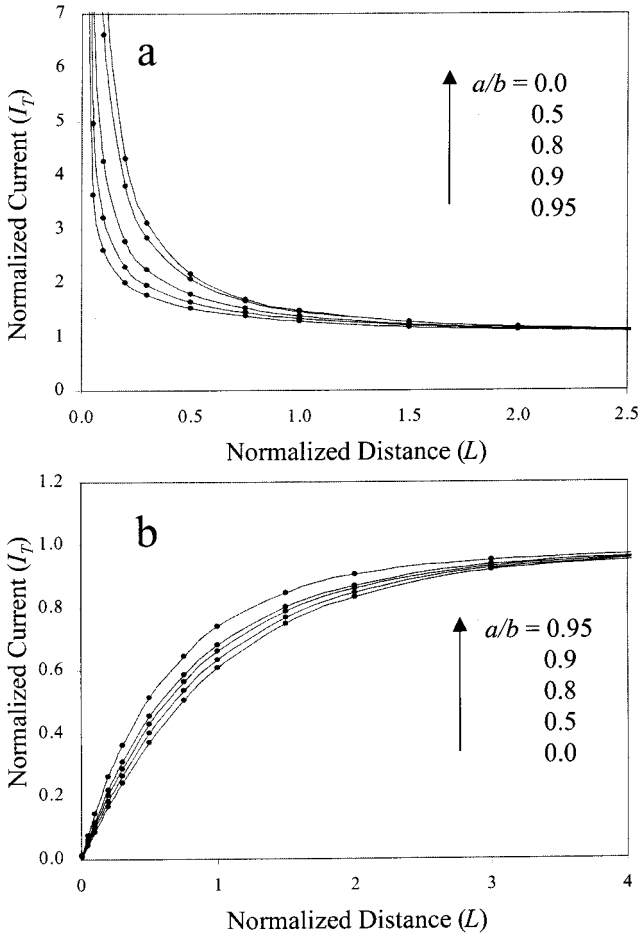

Figure 2. Theoretical SECM feedback responses of ring microelectrodes at (a) conductive and (b) insulating substrates with various a/b ratios while RG = 5.

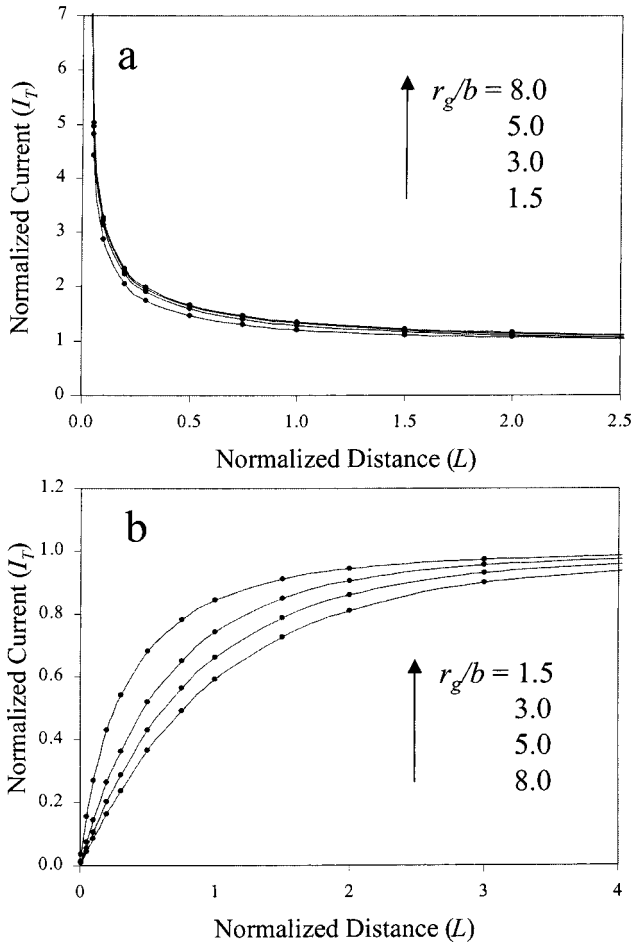

Figure 3. Theoretical SECM feedback responses of ring microelectrodes at (a) conductive and (b) insulating substrates with various RG values while a/b = 0.9.

feedback currents for a conductive substrate. For example, ring electrodes with $a/b = 0.95$ need to be positioned at $L \approx 0.2$ to obtain a 2 times enhancement of the feedback current, while disk electrodes reach the same feedback current at $L \approx 0.6$ (Figure 2a). The reason for the relatively smaller feedback at ring electrodes with conductive substrates can be explained as follows. When the electrodes are far from a substrate, the diffusion to electrodes achieves a spherical diffusion layer, whose dimensions are represented by the ring radii (so the behavior is rather disklike). However, when the electrode is very close to a conductive substrate, the diffusion layer is disturbed by the substrate before reaching a spherical diffusion field and the dimensions of the diffusion layer are represented by the ring thickness rather than the ring radius. Thus, the feedback currents decrease as the ring becomes thinner.

For insulating substrates, SECM feedback responses are less dependent on the a/b ratio compared to conductive substrates (Figure 2b). For example, when $a/b = 0.95$, the maximum deviation from the SECM curves for disk electrodes was less than 30%. When the SECM tip is positioned close to an insulating substrate, the substrate hinders the diffusion of species O from the bulk solution to the electrode surface; therefore, the tip current is lower than $i_{T,\infty}$ (negative feedback). Since the surface of disk electrodes is not uniformly accessible, most of O that diffuses from the bulk solution is reduced at the edge of the electrode; that is, the current density at the edge of the disk is higher than that in the center. Ring electrodes have higher current densities than disk electrodes due to the extra inner edge, which allow the study of the faster electrode reactions.[38,39] At close proximity, the contribution of the reduction of O at the outer edge of the electrodes is more important, because the diffusion to the center of the electrode is disturbed by the insulating substrate. In other words, most O is reduced at the outer edge. Thus, the SECM approach curves are not strongly influenced by the a/b ratio, if the size of the outer circumference is the same.

Effect of Insulating Sheath Thickness on SECM Approach Curves. Most previous SECM studies assume a thick insulating sheath compared to the electrode area; the most commonly used RG value is 10. However, in practice the thickness is usually smaller, particularly in the tips described here and used with optical measurements. To study the effect of RG on the SECM feedback response for a ring electrode, theoretical SECM curves with different RG values and an a/b ratio fixed to 0.9 were obtained (Figure 3). As reported for disk electrodes, RG values affect the SECM curves for insulating substrates more obviously than for

(38) Wightman, R. M.; Wipf, D. O. In *Electroanalytical Chemistry*; Bard, A. J., Ed.; Marcel Dekker: New York, 1988; Vol. 15, p 267.
(39) Russell, A.; Repka, K.; Dibble, T.; Ghoroghchian, J.; Smith, J. J.; Fleischmann, M.; Pitt, C. H.; Pons, S. *Anal. Chem.* **1986**, *58*, 2961.

conductive substrates. With insulating substrates, a smaller RG value results in a higher current at any distance between tip and substrate, since the contribution of mediator diffusion from behind the shield is not negligible when the thickness of insulator shield is thin. However, the SECM approach curve for a conductive substrate does not vary much with RG value, since the diffusion of O from bulk solution to electrode surface makes a smaller contribution to the tip current. As the insulating sheath becomes thinner, $i_{T,\infty}$ increases and the normalized feedback currents decrease. Thus, slightly less feedback enhancements are observed as RG values decrease.

Thus, information about the a/b ratio of ring electrodes can be extracted by analyzing SECM curves at conductive substrates, because these only weakly depend on RG values. RG values can be obtained by studying SECM curves at insulating substrates, where there is a strong dependency on the thickness of insulating sheath.

Determination of the Tip Geometry, Inner and Outer Radii of a Ring, and Thickness of the Insulating Sheath. We now discuss the application of the theoretical curves to the experimental determination of the geometry of ring electrodes prepared by pulling optical fibers, depositing gold, and insulating with electrophoretic paint. This is based on the measured $i_{T,\infty}$ value and a comparison of the theoretical and experimental SECM curves at both conductive and insulating substrates. The iterative procedure used to determine tip geometry is shown as a flowchart in Figure 4.

An initial estimate of electrode size can be made from the measured $i_{T,\infty}$. For a/b ratios that were within a reasonable range (as estimated from microscopy), the numerical difference of $i_{T,\infty}$ for ring-shaped and disk-shaped electrodes can be estimated from Table 2. For example, when $a/b = 0.95$, $i_{T,\infty}$ (*ring*) is only 73% of $i_{T,\infty}$ (*disk*). In other words, a ring-shaped electrode with inner radius a and outer radius b results in a 27% smaller current than a disk-shaped electrode with the same radius b. From this we can estimate the current of disk electrodes whose diameters are the same as the outer diameters of ring electrodes for each chosen a/b. The current at a disk electrode is given by

$$i_{T,\infty}(\text{disk}) = 4nFDc_0b \qquad (15)$$

Thus, we can estimate a value of b from the steady-state current for a disk-shaped electrode using this equation. The a/b ratio and the obtained value of b in each calculation also allows an estimation of a. In the case of a ring electrode used in this study, $i_{T,\infty}$ (ring) was 8.1 nA. Therefore, with 0.95 as the a/b ratio, the estimated $i_{T,\infty}$ (disk), b, and a were 11 nA, 2.15 μm, and 2.05 μm, respectively. Using the value of b and experimental $i_{T,\infty}$, we can normalize the experimental SECM approach curves over conductive substrates; the normalized current is $i_T/i_{T,\infty}$ and the normalized distance is d/b.

As discussed above, the SECM curves for conductive substrates depend on the a/b ratio much more strongly than the RG value. Thus, it is possible to find the optimum value for the a/b ratio by observing the best fit between the normalized experimental and the normalized theoretical SECM approach curves at conductive substrates. The experimental curves for a given a/b ratio were compared to the calculated theoretical curves for the same a/b ratio with RG fixed at 5. RG = 5 was chosen as a preliminary estimate rather than any larger number because we knew from the tip preparation method and microscopic observation of the tip that it could not be larger than this value. The a/b value was changed and the experimental and theoretical curves were compared until the best fit was obtained. This then allowed determination of a and b, based on the known value of $i_{T,\infty}$. SECM approach curves for conductive substrates were quite sensitive to the ratio of a/b, and it was reasonably straightforward to extract the value of a/b by fitting the experimental to theoretical curves. These fittings for our electrode are shown in Figure 5 and demonstrate that this fitting procedure is sensitive enough to allow

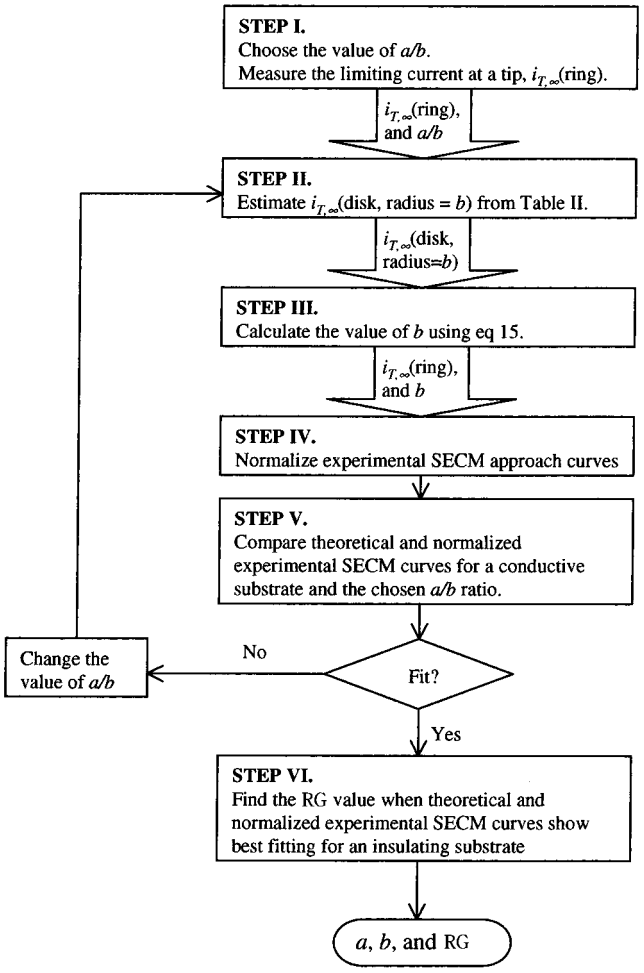

Figure 4. Procedure to determine the values of a, b, and RG of ring microelectrodes.

Table 2. Normalized Current for Different Values of a/b When RG = 5

a/b	$i_{T,\infty}$(ring)/$i_{T,\infty}$(disk)	a/b	$i_{T,\infty}$(ring)/$i_{T,\infty}$(disk)
0[a]	1.000	0.7	0.933
0.2	0.998	0.8	0.888
0.3	0.988	0.9	0.816
0.4	0.979	0.95	0.727
0.5	0.978	0.98	0.636
0.6	0.961	0.99	0.539

[a] When $a/b = 0$, the shape of the electrode is a disk.

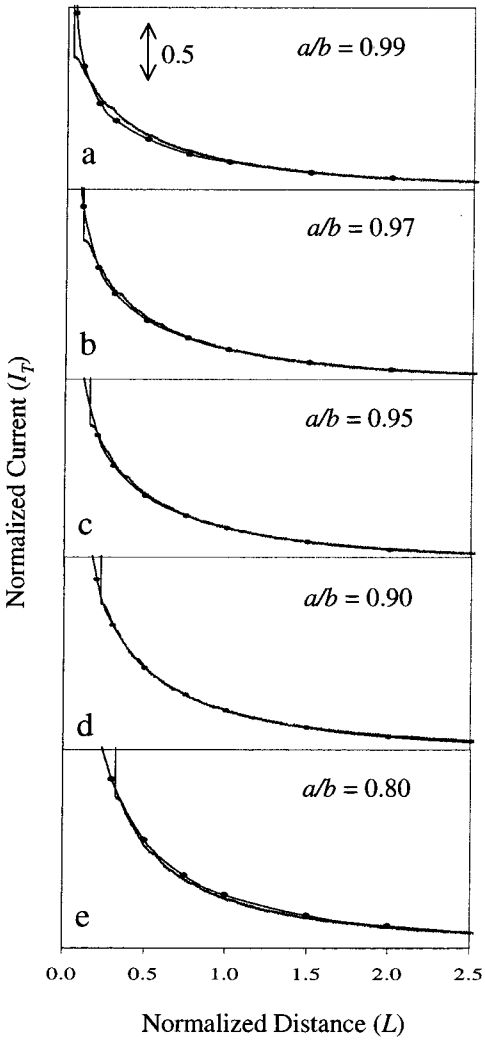

Figure 5. Comparison of the theoretical and experimental SECM curves at conductive substrates at the indicated *a*/*b* ratios while RG = 5. Theoretical curves (dotted lines) and normalized experimental curves (solid lines) over Pt substrate in an aqueous solution containing 20 mM $Ru(NH_3)_6^{3+}$ and 0.1 M KCl.

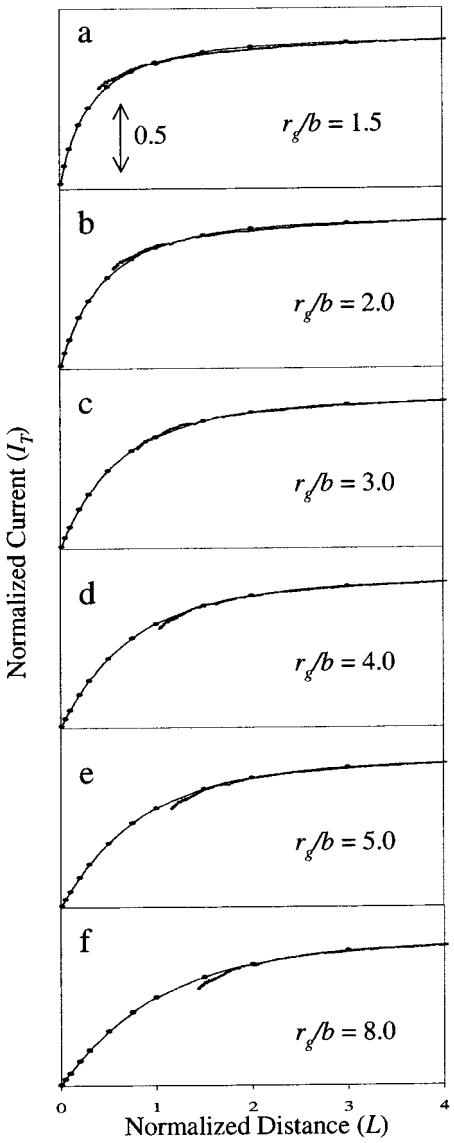

Figure 6. Comparison of the experimental SECM curve to theoretical ones for an insulating substrate for different values of RG: (a) 1.5, (b) 2, (c) 3, (d) 4, (e) 5, and (f) 8 while the *a*/*b* ratio = 0.9. Theoretical curves (dotted lines) and normalized experimental curve (solid line) for a glass substrate in an aqueous solution containing 20 mM $Ru(NH_3)_6^{3+}$ and 0.1 M KCl. The best fit was obtained with RG = 3.

determination of the a/b ratio. The fitting curves were obtained with different a/b ratios, and the normalized experimental curves deviated slightly from the theoretical curves in all cases other than $a/b = 0.9$.

For insulating substrates, the important factor in the determination of the SECM approach curves is the RG value rather than the a/b ratio. Thus, information about the RG value can be obtained from approach curves with insulating substrates. The experimental SECM curves were normalized using the experimental $i_{T,\infty}$, and the value of b was optimized from the case of conductive substrates. After normalization, this curve was compared with the normalized theoretical SECM approach curves for $a/b = 0.9$ obtained with insulating substrates, while the value of RG was varied (Figure 6). As with conductive substrates, the SECM approach curves were sensitive to the value of RG and the best fit allows determination of the thickness of insulating sheath.

In the overall procedure to determine a, b, and RG, the most important step was to take the optimum number for the ratio of a/b. The three parameters obtained for the tips used in this study were $a = 1.50-1.70$ μm, $b = 1.67-1.89$ μm, and RG = 2−3. The thickness of a gold ring was thus ~200 nm. Although the RG value obtained at insulating substrates (3) was different from the value used in the case of conductive substrates (5) this difference is not important, because the SECM curves for conductive substrates are not very sensitive to the RG value. In the final refitting, the experimental curves agreed very well with the theoretical ones for a conductive substrate (Figure 7).

CONCLUSIONS

Theoretical SECM tip current−distance curves for ring electrodes were calculated by numerical analysis using PDEase2D, a software program employing finite element analysis. The diffusion-limited steady-state currents of ring microelectrodes were calculated at various distances (L) between an electrode and conductive

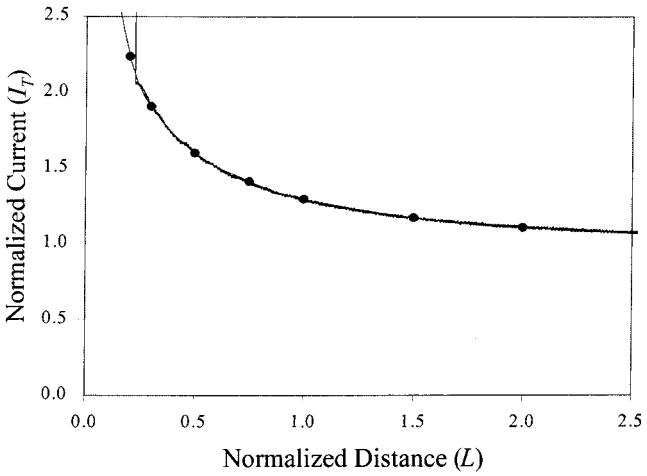

Figure 7. Comparison of the theoretical and experimental SECM curves at conductive substrates. $a/b = 0.90$ and RG = 3. Theoretical curves (dotted lines) and normalized experimental curves (solid lines) over Pt substrate in an aqueous solution containing 20 mM $Ru(NH_3)_6^{3+}$ and 0.1 M KCl.

or insulating substrates. When the electrodes are positioned far from substrates, the calculated currents ($i_{T,\infty}$) showed a strong dependence on the ratio of the inner/outer ring radii and on the thickness of insulating sheath. These results agreed well with previous ones for ring electrodes, thus providing confidence in the reliability of the simulation.

The theoretical SECM curves at conductive substrates were influenced significantly by a/b ratio but only slightly by the thickness of insulating sheath. They showed that the positive feedback effect with a ring microelectrode is less than that of a disk microelectrode; that is, as the ring becomes thinner, the extent of positive feedback decreases. On the other hand, SECM curves at insulating substrates depend on the RG value rather than the a/b ratio. Indeed, they are very similar to those of disk microelectrodes as long as the RG value is constant. The fact that SECM responses for ring microelectrodes at conductive and insulating substrates were sensitive to one of two parameters in each case instead of both, allowed us to determine the geometry of ring electrodes using SECM curves. Dependency of SECM curves on the a/b ratio or the RG value in each case allowed the determination of the three parameters, a, b, and r_g by an iterative procedure. In fact, information about a and b is largely obtained from $i_{T,\infty}$ and the SECM curves at conductive substrates, while the r_g value was extracted from the SECM curves at insulating substrates (by comparison of experimental and theoretical curves). The obtained values of a, b, and r_g for the ring microelectrodes based on pulled optical fibers were 1.7, 1.9, and 5.7 μm, respectively.

Received for review December 12, 2000. Accepted March 1, 2001.

AC0014764